Available online at www.sciencedirect.com
SCIENCE DIRECT®
Journal of Computational Physics 195 (2004) 341–354
JOURNAL OF COMPUTATIONAL PHYSICS
www.elsevier.com/locate/jcp

Eddy viscosity of cellular flows by upscaling

Alexei Novikov [1]

Applied and Computational Mathematics, California Institute of Technology, 1200 E California Boulevard, MC 217-50, Pasadena, CA 91125, USA

Received 28 November 2002; received in revised form 12 August 2003; accepted 3 October 2003

Abstract

The eddy viscosity is the tensor in the equation that governs the transport of the large-scale (modulational) perturbations of small-scale stationary flows. As an approximation to eddy viscosity the effective tensor, that arises in the limit as the ratio between the scales $\varepsilon \to 0$, can be considered. We are interested here in the accuracy of this approximation. We present results of computational investigation of eddy viscosity, when the small-scale flows are cellular, special periodic stationary flows with the stream function $\phi = \sin y_1 \sin y_2 + \delta \cos y_1 \cos y_2$, $y = x/\varepsilon$, $0 \leqslant \delta \leqslant 1$. For small ε we used a numerical upscaling method. We designed this method so that it captures the modulational perturbations for any ε with $O(\varepsilon^2)$ accuracy and independent of ε complexity.

Keywords: Eddy viscosity; Upscaling; Computational fluid dynamics

1. Formulation

For incompressible highly oscillatory small-scale flow v subject to forcing periodic in space and time the eddy viscosity, which controls the large-scale transport of momentum, can be determined in a systematic way by multiscale analysis (see e.g. [3,12–14]). More specifically, assume that v is modeled as a stationary solution of the Navier–Stokes equations with some auxiliary forcing

$$v \cdot \nabla v = \nu \Delta v - \nabla p + f, \quad \nabla \cdot v = 0.$$

The role of the forcing is to sustain the flow pattern of v, and its detailed structure is not of interest. If v is modulated initially by a large-scale flow, then, due to nonlinear coupling in the Navier–Stokes equations, the modulational perturbation u has the large-scale part $\langle u \rangle(t,x)$ and a small-scale part $u_s = u_s(\langle u \rangle, v)$. The coupling between u_s and v gives rise to eddy viscosity.

E-mail address: anovikov@math.psu.edu (A. Novikov).
[1] Present address: Department of Mathematics, Penn State University, University Park, PA 16802, USA.

0021-9991/$ - see front matter © 2003 Elsevier Inc. All rights reserved.
doi:10.1016/j.jcp.2003.10.003

Consider a special case. On a periodic square domain $\Omega = [0, 2\pi] \times [0, 2\pi]$ with periodic boundary conditions the underlying family of $2\pi\varepsilon$-periodic stationary flows $v^\varepsilon(x/\varepsilon)$ are *cellular*:

$$v^\varepsilon\left(\frac{x}{\varepsilon}\right) = \frac{1}{\varepsilon} v(y), \quad y = x/\varepsilon, \quad v(y) = \left(-\frac{\partial}{\partial y_2}\phi, \frac{\partial}{\partial y_1}\phi \right),$$
$$\phi(y) = \sin y_1 \sin y_2 + \delta \cos y_1 \cos y_2, \quad 0 \leqslant \delta \leqslant 1. \tag{1}$$

The scaling of v^ε is chosen so that the Reynolds number associated with v^ε is a constant, independent of ε:

$$Re = \frac{\max |v^\varepsilon| 2\pi\varepsilon}{\nu} = C \max |v^\varepsilon(x/\varepsilon)|\varepsilon = C \max |v(x/\varepsilon)|.$$

Cellular flows is a special class of stationary solutions of the Euler equations in two dimensions, because they satisfy

$$\Delta v^\varepsilon\left(\frac{x}{\varepsilon}\right) = -\frac{\kappa}{\varepsilon^2} v^\varepsilon\left(\frac{x}{\varepsilon}\right) \tag{2}$$

with $\kappa = 2$, which is a two-dimensional *analog* of the Beltrami property (for the usual Beltrami property see e.g. [1]). The parameter δ characterizes the size of channels of v^ε. If $\delta = 0$, then there is no channels – the motion of fluid parcels is contained in small boxes of size $\approx \varepsilon \times \varepsilon$. Such flows are known as two-dimensional Taylor–Green flows. If $\delta > 0$ then there are channels (see Fig. 1), that allow some fluid parcels to travel along the flow whereas other fluid parcels are contained in islands of size $\approx \varepsilon \times \varepsilon$. Such flows are known as cat's-eye flows. If $\delta = 1$, then the islands disappear and we have a pure periodic shear flow. If v^ε is modulated initially by $u_0(x)$, then the equation for the modulational perturbation u^ε can be conveniently written for its vorticity ω^ε as (for details see [9,10])

$$\partial_t \omega^\varepsilon + \frac{1}{\varepsilon} v\left(\frac{x}{\varepsilon}\right) \cdot \nabla S^\varepsilon(\omega^\varepsilon) + u^\varepsilon \cdot \nabla \omega^\varepsilon = \frac{1}{Re} \Delta \omega^\varepsilon, \quad \nabla \cdot v = 0, \quad \nabla \cdot u^\varepsilon = 0, \quad \omega^\varepsilon = \nabla \times u^\varepsilon,$$
$$\omega^\varepsilon(0, x) = \omega_0(x) = \nabla \times u_0(x),$$

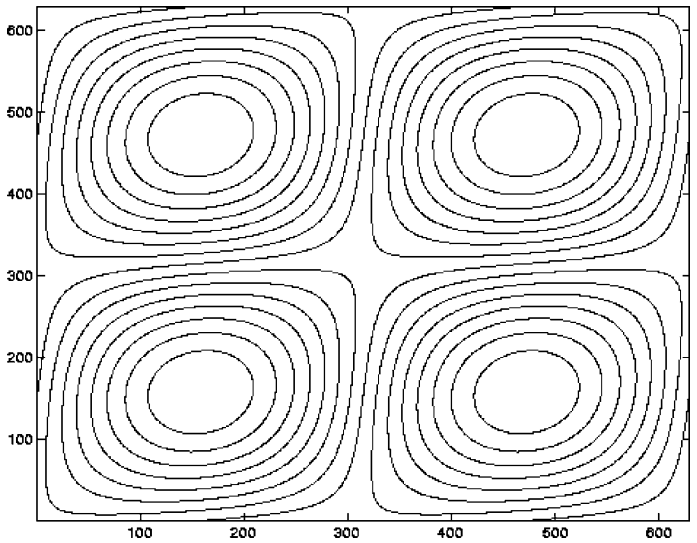

Fig. 1. Level sets of the stream function of cellular flows with small channels, $\delta = 0.1$.

where

$$S^{\varepsilon}(\omega^{\varepsilon}) = \left(\Delta + \frac{2}{\varepsilon^2}\right)\Delta^{-1}\omega^{\varepsilon}.$$

The operator S^{ε} is well defined on mean-zero periodic functions, provided $\varepsilon = 1/k$, $k \in \mathbb{Z}$ and

$$\int_{\Omega} \omega^{\varepsilon}(x,t)\mathrm{d}x = 0.$$

Using multiscale asymptotics (see e.g. [2]) the effective modulation equation in the limit $\varepsilon \to 0$ is computed in [10]. It also was shown in [10] that

- eddy viscosity arises from

$$\frac{1}{\varepsilon} v\left(\frac{x}{\varepsilon}\right) \cdot \nabla S^{\varepsilon}(\omega^{\varepsilon})$$

  only,
- the nonlinear term

$$u^{\varepsilon} \cdot \nabla \omega^{\varepsilon}$$

  converges, as $\varepsilon \to 0$, to a nonlinear operator that does not affect the stability of the solutions of the effective equation.

Therefore for the study of eddy viscosity effects it is sufficient to analyze the linearized case, where the vorticity of the modulational perturbation satisfies

$$\begin{aligned} &\partial_t \omega^{\varepsilon} + \frac{1}{\varepsilon} v\left(\frac{x}{\varepsilon}\right) \cdot \nabla S^{\varepsilon}(\omega^{\varepsilon}) = \frac{1}{Re}\Delta\omega^{\varepsilon}, \\ &\nabla \cdot v = 0, \\ &\omega^{\varepsilon}(0,x) = \omega_0(x). \end{aligned} \tag{3}$$

In this work, we study Eq. (3) only. In the linearized case, the effective modulation equation is

$$\begin{aligned} &\partial_t \omega = \frac{1}{Re}\Delta\omega + M\omega, \\ &\omega(0,x) = \omega_0(x), \end{aligned} \tag{4}$$

where

$$\begin{aligned} &M\omega = -\frac{Re}{8}((\nabla_1 + \delta\nabla_2)^2 + (\delta\nabla_1 + \nabla_2)^2)\omega + \left(\frac{Re}{2}(1+\delta^2) + \nu'\right)(\nabla_2^2 - \nabla_1^2)^2\Delta^{-1}\omega, \\ &\nabla_i = \frac{\partial}{\partial x_i}, \quad i = 1,2. \end{aligned} \tag{5}$$

The constant ν' in the equation for M satisfies $\nu' \geqslant 0$, $\nu' = \nu'(Re,\delta)$, and can be computed numerically using the solution of a periodic boundary value (cell) problem (see [10]).

The eddy viscosity of cellular flows determines the behavior of solutions of (3). An approximate behavior of these solutions can be predicted by the solutions of the effective modulation Eq. (4). The main issue we address in this work is the accuracy of this prediction. More specifically, the predictions of the effective theory can be analyzed by the plane waves

$$\omega = a(t)\exp(\mathrm{i}m \cdot x), \quad a(0) = 1, \quad m = (m_1, m_2),$$

which are the exact solutions of the effective Eq. (4). The dispersion relations of these plane wave solutions can be found using (4) with (5), and they give that the amplitude of these solutions

$$a(t) = \exp \sigma t,$$

where $\sigma = \sigma(m, \delta, Re)$ crucially depends on the chosen Reynolds number Re, wave-vector m, and size of channels δ. In this paper for different values of ε, Re, m and δ we compute with $O(\varepsilon^2)$ accuracy the numerical error between the plane wave solutions of the effective Eq. (4) and the corresponding solutions of (3) with the initial conditions

$$\omega^\varepsilon(0,x) = \omega(0,x) = \exp(\mathrm{i}m \cdot x), \quad m = (m_1, m_2).$$

The large scales in our problem are determined by the initial conditions. Rigorously this can be defined by means of a projection operator

$$\langle \cdot \rangle : \omega^\varepsilon(t,x) \to \langle \omega^\varepsilon \rangle(t,x)$$

on the space of finite trigonometric polynomials

$$\int_\Omega \exp(\mathrm{i}m \cdot x) \langle \omega^\varepsilon \rangle(t,x) \mathrm{d}x = \begin{cases} \int_\Omega \exp(\mathrm{i}m \cdot x) \omega^\varepsilon(t,x) \mathrm{d}x & \text{if } |m| \leqslant K, \\ 0 & \text{otherwise,} \end{cases}$$

where a fixed constant K is chosen so that the initial conditions are large scale

$$\langle \omega^\varepsilon(0,x) \rangle \equiv \omega^\varepsilon(0,x).$$

The small scales are defined by the projection operator $\mathbb{P}_s$ on the orthogonal complement of the space of finite trigonometric polynomials

$$\mathbb{P}_s(\omega^\varepsilon) = \omega^\varepsilon - \langle \omega^\varepsilon \rangle.$$

These definitions are more convenient for our problem; however, they are equivalent to standard ones (see e.g. [2]).

Our main numerical technique is upscaling. Generally, the idea of upscaling (see e.g. [15]) is to reformulate the original problem so that large time-steps can be taken in order to capture accurately the behavior of the mean flow with an $O(\varepsilon)$ error. For our purposes such accuracy in ε is insufficient. Therefore by upscaling we mean a numerical method with complexity independent of ε, that captures accurately the behavior of the mean flow $\langle \omega^\varepsilon \rangle$ with an $O(\varepsilon^2)$ error. The main issue here is to account for possible accumulation of $O(\varepsilon)$ error while time-stepping.

The paper is organized as follows. We first describe the design of our upscaling method, then give details of its implementation for cellular flows, then mention the numerical algorithms used in obtaining the numerical results, which we present in the end.

2. Upscaling

Our Eq. (3) is very similar to the convection–diffusion of a passive scalar

$$\partial_t \omega^\varepsilon(x,t) + \frac{1}{\varepsilon} v\left(\frac{x}{\varepsilon}\right) \cdot \nabla \omega^\varepsilon(x,t) = \frac{1}{Pe} \Delta \omega^\varepsilon(x,t), \quad \nabla \cdot v = 0, \tag{6}$$

where the Péclet number

$$Pe = \frac{\max |v|}{\sigma},$$

σ is the diffusivity of the passive scalar ω^ε.

The convection–diffusion equation of a passive scalar for large Péclet number has been studied for cellular flows in [5] (for random flows see e.g. [4] and references therein). It was shown in [5], that if the passive scalar ω^ε is decomposed into a smooth mean part and a highly oscillatory mean-zero part

$$\omega^\varepsilon = \langle \omega^\varepsilon \rangle + \omega^\varepsilon_{\mathrm{s}}, \quad \langle \omega^\varepsilon_{\mathrm{s}} \rangle = 0, \tag{7}$$

then

$$\partial_t \langle \omega^\varepsilon \rangle + \frac{1}{\varepsilon} \left\langle v\left(\frac{x}{\varepsilon}\right) \cdot \nabla \omega^\varepsilon_{\mathrm{s}} \right\rangle = \frac{1}{Pe} \Delta \langle \omega^\varepsilon \rangle, \quad \nabla \cdot v = 0, \tag{8}$$

$$\omega^\varepsilon_{\mathrm{s}} = \varepsilon \omega_1 + \varepsilon^2 \omega_2 + \varepsilon^3 \omega_3 + \cdots,$$

$$\partial_t \omega^\varepsilon_{\mathrm{s}} = \mathrm{O}(\varepsilon) \text{ and therefore } \mathbb{P}_{\mathrm{s}} \left[\frac{1}{Pe} \Delta - \frac{1}{\varepsilon} v\left(\frac{x}{\varepsilon}\right) \cdot \nabla \right]^{-1} \partial_t \omega^\varepsilon_{\mathrm{s}} = \mathrm{O}(\varepsilon^3).$$

This implies two scaling observations. The first is that

$$\frac{1}{\varepsilon} \langle v \cdot \nabla \omega^\varepsilon_{\mathrm{s}} \rangle$$

can be computed with an $\mathrm{O}(\varepsilon^2)$ error, if $\omega^\varepsilon_{\mathrm{s}}$ is resolved with an $\mathrm{O}(\varepsilon^3)$ error. The second is that $\omega^\varepsilon_{\mathrm{s}}$ can be resolved with an $\mathrm{O}(\varepsilon^3)$ error if we neglect $\partial_t \omega^\varepsilon_{\mathrm{s}}$, because, subtracting (8) from (6) and resolving for $\omega^\varepsilon_{\mathrm{s}}$ we have

$$\begin{aligned} \omega^\varepsilon_{\mathrm{s}} &= \mathbb{P}_{\mathrm{s}} \left[\frac{1}{Pe} \Delta - \frac{1}{\varepsilon} v\left(\frac{x}{\varepsilon}\right) \cdot \nabla \right]^{-1} \mathbb{P}_{\mathrm{s}} \left[\frac{1}{\varepsilon} v\left(\frac{x}{\varepsilon}\right) \cdot \nabla \langle \omega^\varepsilon \rangle \right] + \mathbb{P}_{\mathrm{s}} \left[\frac{1}{Pe} \Delta - \frac{1}{\varepsilon} v\left(\frac{x}{\varepsilon}\right) \cdot \nabla \right]^{-1} \partial_t \omega^\varepsilon_{\mathrm{s}} \\ &= \mathbb{P}_{\mathrm{s}} \left[\frac{1}{Pe} \Delta - \frac{1}{\varepsilon} v\left(\frac{x}{\varepsilon}\right) \cdot \nabla \right]^{-1} \mathbb{P}_{\mathrm{s}} \left[\frac{1}{\varepsilon} v\left(\frac{x}{\varepsilon}\right) \cdot \nabla \langle \omega^\varepsilon \rangle \right] + \mathrm{O}(\varepsilon^3). \end{aligned}$$

This key observation means that a sufficiently well-resolved $\omega^\varepsilon_{\mathrm{s}}$ can be found by accurate upscaling methods for elliptic problems (see e.g. [7]).

Hence, an upscaling method for convection–diffusion equation can be designed as follows. Solve the elliptic problem

$$\mathbb{P}_{\mathrm{s}} \left[\frac{1}{Pe} \Delta - \frac{1}{\varepsilon} v\left(\frac{x}{\varepsilon}\right) \cdot \nabla \right] \omega^\varepsilon_{\mathrm{s}} = \mathbb{P}_{\mathrm{s}} \left[\frac{1}{\varepsilon} v\left(\frac{x}{\varepsilon}\right) \cdot \nabla \langle \omega^\varepsilon \rangle \right] \tag{9}$$

using, for example, methods of [7]. Then perform a time-step only for the mean flow $\langle \omega^\varepsilon \rangle$ using (8), then update $\omega^\varepsilon_{\mathrm{s}}$ using (9), then perform the next time-step. Note, that if $\langle \omega^\varepsilon \rangle$ and $\omega^\varepsilon_{\mathrm{s}}$ solve (8) and (9), ω^ε solves (6), then, instead of (7), we have

$$\omega^\varepsilon = \langle \omega^\varepsilon \rangle + \omega^\varepsilon_{\mathrm{s}} + \mathrm{O}(\varepsilon^2),$$

as $\varepsilon \to 0$. The CFL condition of (8) is independent of ε, therefore this numerical method is upscaling.

In the convection–diffusion case the $\mathrm{O}(\varepsilon^2)$ accuracy of the upscaling is achieved without resolving $\partial_t \omega^\varepsilon_{\mathrm{s}}$. In the case of eddy viscosity (3), analysis shows (see [9]) that, after the decomposition of ω^ε as in (7), $\omega^\varepsilon_{\mathrm{s}}$ has the expansion

$$\omega^\varepsilon_{\mathrm{s}} = \frac{1}{\varepsilon} \omega_1 + \omega_2 + \varepsilon \omega_3 + \varepsilon^2 \omega_4 + \cdots, \tag{10}$$

and

$$\partial_t \omega_s^\varepsilon = O(\varepsilon^{-1}), \quad \partial_t \left[\partial_t \bar{\omega}^\varepsilon \right] = O(\varepsilon^{-1}).$$

In contrast to the convection–diffusion case, the two scaling observations here are different. The first is that

$$\frac{1}{\varepsilon} \langle v \cdot \nabla S^\varepsilon \omega_s^\varepsilon \rangle$$

can be computed with an $O(\varepsilon^2)$ error, if ω_s^ε is resolved with an $O(\varepsilon^2)$ error, hence in the expansion (10) three terms $\omega_1, \omega_2, \omega_3$ need to be determined. In order to see that multiply $v \cdot \nabla S^\varepsilon \omega_s^\varepsilon$ by a large-scale test-function $\chi(x)$, $\langle \chi \rangle = \chi(x)$, integrate by parts

$$\langle \chi, v \cdot \nabla S^\varepsilon \omega_s^\varepsilon \rangle \equiv -\langle \omega_s^\varepsilon, S^\varepsilon v \cdot \nabla \chi \rangle,$$

and observe that if $\chi = O(1)$, then $S^\varepsilon v \cdot \nabla \chi = O(\varepsilon)$. The second observation is that $\partial_t \omega_s^\varepsilon$ needs to be resolved with an $O(1)$ error. Hence $\partial_t \omega_s^\varepsilon$ cannot be ignored in upscaling.

Consider another decomposition

$$\omega^\varepsilon = \langle \omega^\varepsilon \rangle + \omega_s^\varepsilon, \quad \omega_s^\varepsilon = \bar{\omega}^\varepsilon + \tilde{\omega}^\varepsilon,$$

where $\bar{\omega}^\varepsilon$ solves the heat equation with forcing

$$\partial_t \bar{\omega}^\varepsilon = \frac{1}{Re} \Delta \bar{\omega}^\varepsilon - \frac{1}{\varepsilon} v\left(\frac{x}{\varepsilon}\right) \cdot \nabla S^\varepsilon \langle \omega^\varepsilon \rangle. \tag{11}$$

Then the analysis of [9] gives that

$$\bar{\omega}^\varepsilon = \frac{1}{\varepsilon} \bar{\omega}_1 + \bar{\omega}_2 + \varepsilon \bar{\omega}_3 + \cdots, \quad \tilde{\omega}^\varepsilon = \tilde{\omega}_1 + \varepsilon \tilde{\omega}_2 + \cdots,$$

and therefore for upscaling we need to resolve the first three terms of $\bar{\omega}^\varepsilon$, but only two terms of $\tilde{\omega}^\varepsilon$.

Similar to the convection–diffusion case, a sufficiently accurate approximation to $\tilde{\omega}^\varepsilon$ can be found as the solution to the time-independent elliptic (cell) problem

$$\mathbb{P}_s \left[\frac{1}{Re} \Delta - \frac{1}{\varepsilon} v\left(\frac{x}{\varepsilon}\right) \cdot \nabla S^\varepsilon \right] \tilde{\omega}^\varepsilon = \mathbb{P}_s \left[\frac{1}{\varepsilon} v\left(\frac{x}{\varepsilon}\right) \cdot \nabla S^\varepsilon (\bar{\omega}^\varepsilon) \right], \tag{12}$$

provided $\bar{\omega}^\varepsilon$ is already determined with $O(\varepsilon^2)$ accuracy.

In order to determine $\bar{\omega}^\varepsilon$ sufficiently accurately, observe that, differentiating (11) with respect to t, we have that $\partial_t \bar{\omega}^\varepsilon$ satisfies

$$\partial_t [\partial_t \bar{\omega}^\varepsilon] = \frac{1}{Re} \Delta [\partial_t \bar{\omega}^\varepsilon] - \frac{1}{\varepsilon} v\left(\frac{x}{\varepsilon}\right) \cdot \nabla S^\varepsilon \partial_t \langle \omega^\varepsilon \rangle.$$

Since

$$\partial_t [\partial_t \bar{\omega}^\varepsilon] = O(\varepsilon^{-1}),$$

we have

$$\partial_t \bar{\omega}^\varepsilon = Re\, \Delta^{-1} \left[\frac{1}{\varepsilon} v\left(\frac{x}{\varepsilon}\right) \cdot \nabla S^\varepsilon \partial_t \langle \omega^\varepsilon \rangle + \partial_t [\partial_t \bar{\omega}^\varepsilon] \right] = \frac{Re}{\varepsilon} \Delta^{-1} \left[v\left(\frac{x}{\varepsilon}\right) \cdot \nabla S^\varepsilon \partial_t \langle \omega^\varepsilon \rangle \right] + O(\varepsilon),$$

and a sufficiently accurate approximation to $\partial_t\bar{\omega}^\varepsilon$ satisfies

$$\partial_t\bar{\omega}^\varepsilon = \frac{Re}{\varepsilon}\Delta^{-1}\left[v\left(\frac{x}{\varepsilon}\right)\cdot\nabla S^\varepsilon\partial_t\langle\omega^\varepsilon\rangle\right].$$

Therefore using (11)

$$\bar{\omega}^\varepsilon = \frac{Re}{\varepsilon}\Delta^{-1}\left(v\left(\frac{x}{\varepsilon}\right)\cdot\nabla S^\varepsilon\langle\omega^\varepsilon\rangle + Re\,\Delta^{-1}\left[v\left(\frac{x}{\varepsilon}\right)\cdot\nabla S^\varepsilon\partial_t\langle\omega^\varepsilon\rangle\right]\right) \tag{13}$$

with an $O(\varepsilon^2)$ error. Hence $\bar{\omega}^\varepsilon$ can be resolved sufficiently accurately, provided we compute the $O(1)$ terms of $\langle\omega^\varepsilon\rangle$ and $\partial_t\langle\omega^\varepsilon\rangle$.

After these preparations the numerical method consists of three alternating parts: evaluate $\bar{\omega}^\varepsilon$ and $\tilde{\omega}^\varepsilon$ using (13) and (12), respectively, and perform a time-step only for the mean flow $\langle\omega^\varepsilon\rangle$ using

$$\partial_t\langle\omega^\varepsilon\rangle + \frac{1}{\varepsilon}\left\langle v\left(\frac{x}{\varepsilon}\right)\cdot\nabla S^\varepsilon(\tilde{\omega}^\varepsilon+\bar{\omega}^\varepsilon)\right\rangle = \frac{1}{Re}\Delta\langle\omega^\varepsilon\rangle, \tag{14}$$

then update $\partial_t\langle\omega^\varepsilon\rangle$ using $\langle\omega^\varepsilon\rangle$ only, then update $\bar{\omega}^\varepsilon$ and $\tilde{\omega}^\varepsilon$ using (13) and (12), then perform the next time-step.

Using an upscaling method for elliptic problems, Eqs. (12) and (13) can be solved accurately with complexity independent of ε, hence our method is upscaling provided the CFL condition of (14) is independent of ε. We claim, that the CFL condition is, indeed, independent of ε; however, it is not immediately obvious. The reason for such favorable CFL condition is the absence of linear anisotropic kinetic alpha (AKA) instabilities (see e.g. [6]) of the underlying flow v. Our flow $v(y)$, $y = x/\varepsilon$ does not have AKA instabilities (see [10]), because it satisfies (2). We discuss the CFL condition in more detail in the next section.

2.1. Implementation for cellular flows

For numerical implementation of our upscaling algorithm for more general flows v^ε, one needs to design effective algorithms to solve elliptic problems (12) and (13). Here we make observations, which are specific to cellular flows. These observations imply that, in our case, a spectral numerical method is a convenient and effective way to solve (12) and (13). The property that the underlying oscillatory flow v^ε is a simple trigonometric polynomial, leads to the following simplifying observations.

If the initial conditions are a single trigonometric function

$$\omega^\varepsilon(x,0) = \exp(\mathrm{i}x\cdot m), \quad m = (m_1,m_2)\in\mathbb{Z}^2, \tag{15}$$

then the solution of (3) for any time has the form

$$\omega^\varepsilon(x,t) = \sum_n a_n^\varepsilon(m,t)\exp(\mathrm{i}(m+n/\varepsilon)\cdot x), \quad n = (n_1,n_2)\in\mathbb{Z}^2. \tag{16}$$

In particular, this means that for any time the mean flow is a plane wave

$$\langle\omega^\varepsilon\rangle(x,t) = a_{oo}^\varepsilon(m,t)\exp(m\cdot x),$$

and it is determined by a single scalar function $a_{oo}^\varepsilon(m,t)$.

The solution to the heat Eq. (11) is a linear combination of four Fourier coefficients

$$\bar{\omega}^\varepsilon(t,x) = \sum_{n=(\pm1,\pm1)} \bar{a}_n^\varepsilon(m,t)\exp(\mathrm{i}(m+n/\varepsilon)\cdot x),$$

where each $\bar{a}^{\varepsilon}_{n}(m,t)$, $n=(\pm1,\pm1)$ satisfies

$$d_t\bar{a}^{\varepsilon}_{\pm1\pm1}(t)=-\frac{1}{Re}\frac{1}{\varepsilon^2}\Delta^{\varepsilon}_{\pm\pm}\bar{a}^{\varepsilon}_{\pm1\pm1}(t)+\frac{1}{\varepsilon^3}\mathbf{C}_{\pm\pm}a^{\varepsilon}(t),\quad \bar{a}^{\varepsilon}_{\pm1\pm1}(0)=0, \tag{17}$$

where $\Delta^{\varepsilon}_{\pm\pm}=2+\varepsilon^2|m|^2+2\varepsilon(\pm m_1\pm m_2)$, and the constants $\mathbf{C}_{\pm\pm}$ are explicitly given by

$$\mathbf{C}_{++}=-\frac{(m_1-m_2)(1-\delta)S}{4},\quad \mathbf{C}_{-+}=\frac{(m_1+m_2)(1+\delta)S}{4},$$

$$\mathbf{C}_{+-}=-\frac{(m_1+m_2)(1+\delta)S}{4},\quad \mathbf{C}_{--}=\frac{(m_1-m_2)(1-\delta)S}{4},$$

where $S=2/(m_1^2+m_2^2)-\epsilon^2$. Therefore the approximation (13) is simply four algebraic equations

$$a^{\varepsilon}_{\pm\pm}(t)=\frac{1}{\varepsilon}\frac{Re\,\mathbf{C}_{\pm\pm}}{\Delta^{\varepsilon}_{\pm\pm}}\left[a^{\varepsilon}_{oo}(t)-\varepsilon^2\frac{Re}{\Delta^{\varepsilon}_{\pm\pm}}d_t a^{\varepsilon}_{oo}(t)\right].$$

If we know explicitly $a^{\varepsilon}_{n}(m,t)$, $n=(\pm1,\pm1)$ for all $t\in[0,T]$, then the mean flow Fourier coefficient $a^{\varepsilon}_{oo}(m,t)$ can be found by solving an ordinary differential equation with forcing determined by $a^{\varepsilon}_{n}(m,t)$, $n=(\pm1,\pm1)$:

$$d_t a^{\varepsilon}_{oo}=-\frac{m^2}{Re}a^{\varepsilon}_{oo}+C_1s_1(t)+C_2s_2(t)+\varepsilon C_3d_1(t)+\varepsilon C_4d_2(t), \tag{18}$$

where

$$C_1=(m_2^2-m_1^2)\frac{1-\delta}{2},\quad C_2=(m_2^2-m_1^2)\frac{1+\delta}{2},\quad C_3=-(m_1-m_2)(m_1^2+m_2^2)\frac{1-\delta}{4},$$
$$C_4=-(m_1+m_2)(m_1^2+m_2^2)\frac{1+\delta}{4},$$

the functions $s_1(t)$, $s_2(t)$ are basically sums and $d_1(t)$, $d_2(t)$ are basically differences of $a^{\varepsilon}_{n}(m,t)$, $n=(\pm1,\pm1)$:

$$\begin{aligned}
s_1(t)&=\frac{a^{\varepsilon}_{11}}{(1+\varepsilon m_1)^2+(1+\varepsilon m_2)^2}+\frac{a^{\varepsilon}_{-1-1}}{(1-\varepsilon m_1)^2+(1-\varepsilon m_2)^2},\\
s_2(t)&=\frac{a^{\varepsilon}_{1-1}}{(1+\varepsilon m_1)^2+(1-\varepsilon m_2)^2}+\frac{a^{\varepsilon}_{-11}}{(1-\varepsilon m_1)^2+(1+\varepsilon m_2)^2},\\
d_1(t)&=\frac{a^{\varepsilon}_{11}}{(1+\varepsilon m_1)^2+(1+\varepsilon m_2)^2}-\frac{a^{\varepsilon}_{-1-1}}{(1-\varepsilon m_1)^2+(1-\varepsilon m_2)^2},\\
d_2(t)&=\frac{a^{\varepsilon}_{1-1}}{(1+\varepsilon m_1)^2+(1-\varepsilon m_2)^2}-\frac{a^{\varepsilon}_{-11}}{(1-\varepsilon m_1)^2+(1+\varepsilon m_2)^2}.
\end{aligned} \tag{19}$$

We intensionally wrote the forcing in terms of s_1, s_2, d_1 and d_2 in order to show how the absence of AKA instabilities is manifested in our case. By (10) $a^{\varepsilon}_{n}(m,t)=O(1/\varepsilon)$, $n=(\pm1,\pm1)$, hence by (18) the CFL condition for (14) is $O(1)$, provided there are symmetries

$$|s_1(t)|\leqslant\varepsilon C|d_1(t)|,\quad |s_2(t)|\leqslant\varepsilon C|d_2(t)|. \tag{20}$$

These symmetries are a consequence of (2), and, for the case of cellular flows, they can be seen in the definition of coefficients $\mathbf{C}_{\pm\pm}$.

In the Fourier space the Eq. (12) is

$$A^{\varepsilon}_{0}\tilde{a}^{\varepsilon}=f^{\varepsilon},$$

where the (infinite-dimensional) matrix A_0^ε with constant coefficients comes from the operator

$$\frac{1}{Re}\Delta - \frac{1}{\varepsilon}v\left(\frac{x}{\varepsilon}\right)\cdot\nabla S^\varepsilon,$$

$\tilde{a}^\varepsilon$ is the (infinite-dimensional) vector of Fourier coefficients of $\tilde{\omega}^\varepsilon$

$$\tilde{\omega}^\varepsilon(x,t) = \sum_n \tilde{a}_n^\varepsilon(m,t)\exp(\mathrm{i}(m+n/\varepsilon)\cdot x), \quad n=(n_1,n_2)\in\mathbb{Z}^2.$$

and the right-hand side f^ε is the vector of Fourier coefficients of

$$\mathbb{P}_s\left[\frac{1}{\varepsilon}v\left(\frac{x}{\varepsilon}\right)\cdot\nabla S^\varepsilon(\bar{\omega}^\varepsilon)\right].$$

The matrix A_0^ε has a simple form. It has diagonal coefficients, that come from the Laplacian and only four other nonzero coefficients in each row/column. The vector f^ε also has only finitely many nonzero entries. In our numerical implementation we approximate $\tilde{a}^\varepsilon$ by its first N Fourier coefficients $\tilde{a}_n^\varepsilon$, $\pi|n|^2\leqslant N$, $N=2Re^2$, approximate A_0^ε by the corresponding $N\times N$ matrix $A=A^\varepsilon$ and find $\tilde{a}^\varepsilon$ as the solution of

$$A\tilde{a}^\varepsilon = f^\varepsilon. \tag{21}$$

It is possible to find $\tilde{a}^\varepsilon$ with any required accuracy by an exponentially converging iteration. In order to observe that decompose A_0^ε into four blocks

$$\begin{pmatrix} A & B\\ C & E\end{pmatrix}\begin{pmatrix}\tilde{a}^\varepsilon_{\mathrm{low}}\\ \tilde{a}^\varepsilon_{\mathrm{high}}\end{pmatrix} = \begin{pmatrix} f^\varepsilon\\ 0\end{pmatrix}, \tag{22}$$

where A is the $N\times N$ matrix from (21), $B=B^\varepsilon$, $C=C^\varepsilon$, $E=E^\varepsilon$ are infinite-dimensional, but B, C have only finitely many nonzero coefficients. Then further decompose

$$E = D + H,$$

where D is the diagonal matrix, that corresponds to the Laplacian, and H has only four nonzero off-diagonal coefficients in each row/column. For our choice of $N=2Re^2$, the diagonal matrix D dominates H, and therefore (see [11]) an accurate approximation to $\tilde{a}^\varepsilon_{\mathrm{high}}$ can be found by an exponentially converging iteration

$$\tilde{a}^\varepsilon_{\mathrm{high},k+1} = -D^{-1}((H+CA^{-1}B)\tilde{a}^\varepsilon_{\mathrm{high},k} + CA^{-1}f^\varepsilon).$$

Therefore, $\tilde{a}^\varepsilon_{\mathrm{low}}$ can be found with any required accuracy as well

$$\tilde{a}^\varepsilon_{\mathrm{low}} = A^{-1}(f^\varepsilon - B\tilde{a}^\varepsilon_{\mathrm{high}}).$$

In our numerical experiments it was observed, however, that for $Re\leqslant 100$, $\tilde{a}^\varepsilon_{\mathrm{high}}$ is negligible – it gives $O(10^{-14})$ correction to the solution of (21).

3. Numerical implementation

In the numerical implementation of upscaling MATLAB is used primarily with the exception of the solution of the linear system (21), where C was used. Time-stepping in (18) for $\langle\omega^\varepsilon\rangle$ is performed by Backward Euler method with variable time-step $\Delta t = .001/\max(1,\ln|a^\varepsilon_{oo}|)$. The four Fourier coefficients of

$\bar{\omega}^\varepsilon$ are determined in terms of sums and differences (19) in order to keep track of symmetries (20). The elliptic problem (12) for $\tilde{\omega}^\varepsilon$ is solved by LU decomposition of (21).

If we say that the result was computed by matrix exponentiation, it means that we approximate the solution of (3) by

$$d_t a^\varepsilon = L^\varepsilon a^\varepsilon, \quad a^\varepsilon(0) = 1, \tag{23}$$

where a^ε are the first N Fourier coefficients of ω^ε, $N = 2Re^2$ and L^ε is a corresponding $N \times N$ matrix of the operator

$$\frac{1}{Re}\Delta - \frac{1}{\varepsilon} v\left(\frac{x}{\varepsilon}\right) \cdot \nabla S^\varepsilon.$$

Then instead of upscaling we use the MATLAB function *expm* for (23).

4. Results

The linearity and scaling arguments (see e.g. [9]) imply that it is sufficient to solve (3) with initial conditions (15), assuming that the wave-vector is normalized to have length 1: $m = (\cos\theta, \sin\theta)$. Our primary interest is the single mean flow Fourier coefficient a^ε_{oo} and its dependence on ε, m, Re, δ. Therefore we present the numerical results for this coefficient only.

The first example was done by matrix exponentiation, because $\varepsilon = 0.25$. In Fig. 2 we plot the value of $a^\varepsilon_{oo}(m,t)$, and the amplitude $a(m,t)$ of the plane wave solution of the effective Eq. (4) for $t = 1$, $Re = 4$ as a function of the channel size $\delta = 0, .1, .2, \ldots, 1$ for five different choices of the wave-vector m:

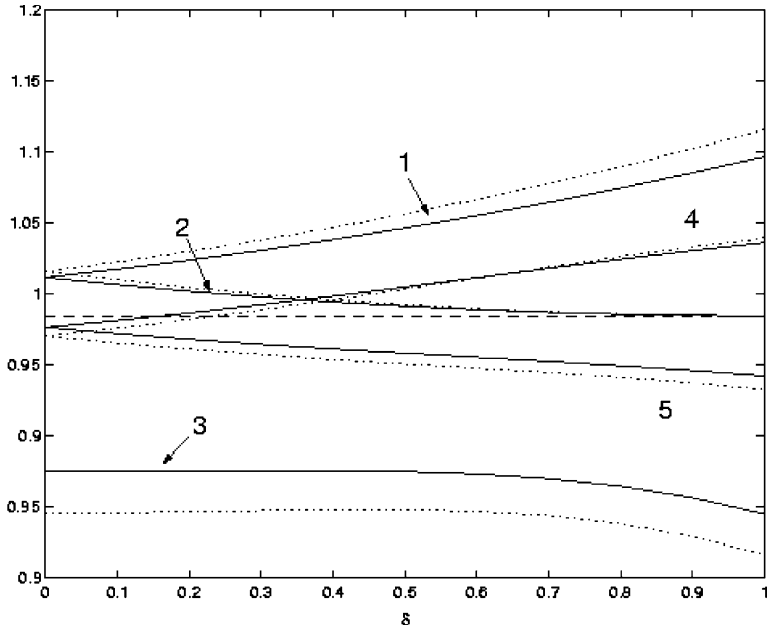

Fig. 2. $Re = 4$, $t = 1$, $\varepsilon = 0.25$. The large-scale Fourier coefficients $a^\varepsilon_{oo}(t)$ (dotted lines) and $a(t)$ (solid lines) as a function of δ for five different choices of the wave-vector m given in Eq. (24). Dashed line is the value of the large-scale Fourier coefficient with no convection term, enhanced/depleted viscosity is below/above this line.

$$
\begin{aligned}
&(1)\quad (m_1, m_2) = (1,1)/\sqrt{2},\\
&(2)\quad (m_1, m_2) = (-1,1)/\sqrt{2},\\
&(3)\quad (m_1, m_2) = (0,1),\\
&(4)\quad (m_1, m_2) = (.5, \sqrt{.75}),\\
&(5)\quad (m_1, m_2) = (-.5, \sqrt{.75}).
\end{aligned}
\tag{24}
$$

The numbering in Fig. 2 corresponds to that of the initial conditions (24). For such small Re and relatively large ε the numerical results agree qualitatively and quantitatively with the effective theory. The results of these numerical experiments confirm the anisotropic tensorial structure of eddy viscosity. Since the dashed line corresponds to the value of the large-scale Fourier coefficient with no convection term, therefore if a curve, or a part of a curve is below the dashed line, then the viscosity is enhanced by the presence of convection; if a curve, or a part of a curve is above the dashed line, then the viscosity is depleted by the presence of convection. Curve 3 corresponds to the case when the plane wave solution of the effective equation is only a function of x_2. The effective theory predicts that this is the case of *maximally enhanced* viscosity for any δ. Curve 1 corresponds to the case when the wave-vector of the plane wave is parallel to the channels. The effective theory predicts that this is the case of *maximally depleted* viscosity. Curve 2 corresponds to the case when the wave-vector is perpendicular to the channels. The effective theory predicts that this is the case of the *maximally depleted* viscosity in the absence of channels ($\delta = 0$); for the shear flows ($\delta = 1$) it predicts that the eddy viscous corrections should not be observable. The initial conditions for curves 4 and 5 are intermediate. We observe depleted viscosity for small channels and enhanced viscosity for large channels for $m = -.5, n = \sqrt{.75}$ (curve 5). The effective theory predicts that for $Re > 2\sqrt{2}/(1+\delta)$ negative eddy viscosity effects should be observed. In our setting it means that a^{ε}_{oo} and a can be larger than 1, for some values of δ and m. We observe it for curves 1, 2, 4.

The second example is done by upscaling for $\varepsilon = .1, .01, .001$ and by matrix exponentiation for $\varepsilon = .1$. Matrix exponentiation method does not converge for $\varepsilon = .01, .001$. It shows that for $Re = 10$ the effective theory could accurately predict the behavior of modulational perturbations if ε is sufficiently small. In particular, $\varepsilon = .1$ is not small enough for this Re. In this experiment we compute the value of $a^{\varepsilon}_{oo}(m,t)$ and $a(m,t)$ for $Re = 10$ as a function of the channel size δ for nine different choices of the wave-vector m:

$$
\begin{aligned}
&m = (0,1), \quad m = (1,1)/\sqrt{2}, \quad m = (-1,1)/\sqrt{2},\\
&m = (.3, \sqrt{1-.3^2}), \quad m = (-.3, \sqrt{1-.3^2}),\\
&m = (.4, \sqrt{1-.4^2}), \quad m = (-.4, \sqrt{1-.4^2}),\\
&m = (.5, \sqrt{1-.5^2}), \quad m = (-.5, \sqrt{1-.5^2}).
\end{aligned}
\tag{25}
$$

A sample of convergence to the effective equations for $\varepsilon = .1$ by matrix exponentiation and for $\varepsilon = .01, .001$ by upscaling is shown in Fig. 3 for $m = (0,1)$, $Re = 10$, $t = 1$ on the log-scale as a function of $\delta = 0, .1, .2, \ldots, 1$. Upscaling for $\varepsilon = .1$ (not shown in Fig. 3) gives that a^{ε}_{oo} is much smaller than the prediction of the effective theory and matrix exponentiation: for $\delta = 0, .1, \ldots, 1$ we have

$$\ln |a^{\varepsilon}_{oo}| \approx -23, -22, -21, -20, -19, -18, -16, -15, -15, -16, -20,$$

respectively. The solid line in Fig. 3 is the prediction of the effective theory, the circles correspond to $\varepsilon = .1$ (matrix exponentiation) and they are significantly far from the solid line. The $\times$ and $+$ symbols correspond to $\varepsilon = .01, .001$ (upscaling), respectively, and they are very close to the solid line. The maximal error

$$e^{\varepsilon} = \max_m |a^{\varepsilon}_{oo}(m,1) - a(m,1)|, \quad \varepsilon = .1, .01, .001,$$

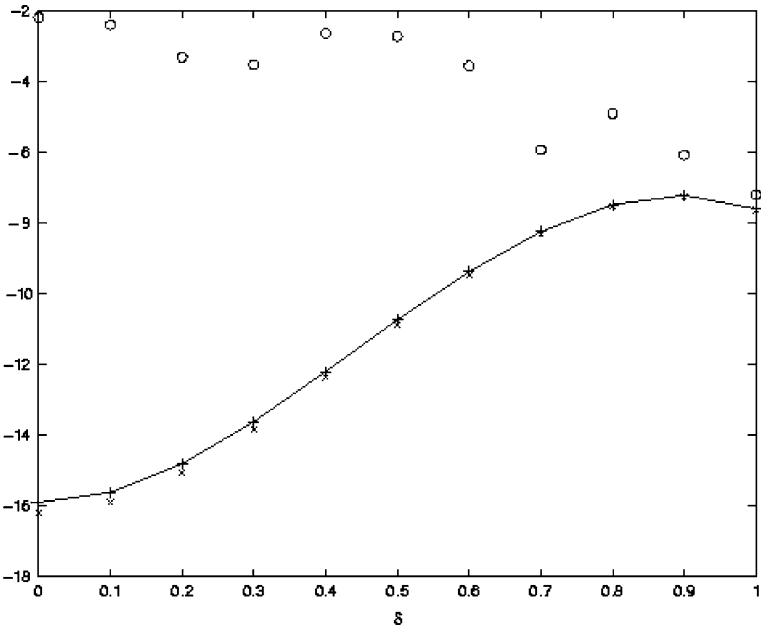

Fig. 3. $Re = 10$, $m = (0,1)$, $t = 1$. Log-scale. The large-scale Fourier coefficients $a^{\varepsilon}_{oo}(t)$ for $\varepsilon = .1$ ($\bigcirc$-line), $\varepsilon = .01$ ($\times$-line), $\varepsilon = .001$ ($+$-line), and the $a(t)$ (solid line) as a function of δ.

for all wave-vectors m determined by (25) is plotted in Fig. 4 on the log-scale as a function of $\delta = 0, .1, .2, \ldots, 1$. Observe, that

$$\log e^{\varepsilon=.01} - \log e^{\varepsilon=.001} \approx 4.6 = 2 \ * \ 2.3 \approx -2\log(.1),$$

hence the error is $O(\varepsilon^2)$. The kinks in the error at $\delta = .3$ in Fig. 4 come from the error of the solution with the wave-vector $m = (-1,1)/\sqrt{2}$. The plane wave solution of the effective equation with this wave-vector changes stability at $\delta \approx .3$: it is unstable (grows exponentially) for $\delta < .3$ and it is stable for $\delta > .3$. Hence, we believe that the explanation for the presence of kinks in Fig. 4 is that the effective equation gives poorer predictions about the solutions of (3) when the plane wave solutions of (4) change stability.

The effective theory predicts that for large Reynolds number there are negative eddy viscosity instabilities for closed cellular flows $\delta = 0$ if the wave-vector $m = (\pm 1, \pm 1)/\sqrt{2}$. The third experiment was done for the wave-vector $m = (1,1)/\sqrt{2}$, $\varepsilon = .01, .001$ and $Re = 1, 2, \ldots, 100$. In Fig. 5 we plot the solution of the effective equation and the *relative* errors

$$r^{\varepsilon} = \frac{|a^{\varepsilon}_{oo}((1,1)/\sqrt{2},1) - a((1,1)/\sqrt{2},1)|}{a((1,1)/\sqrt{2},1)}, \quad \varepsilon = .01, .001,$$

as a function of the Reynolds number on the log-scale. We use here the relative error for convenience of graphical representation of the results. The relative error deteriorates as $Re \to 100$. This can be explained by observation that we neglect $O(\varepsilon^2)$ error. This error becomes significant as $Re \to \infty$. Therefore when $\varepsilon Re = O(1)$ for an accurate solution of (3) asymptotic analysis with two parameters ε and Re is required.

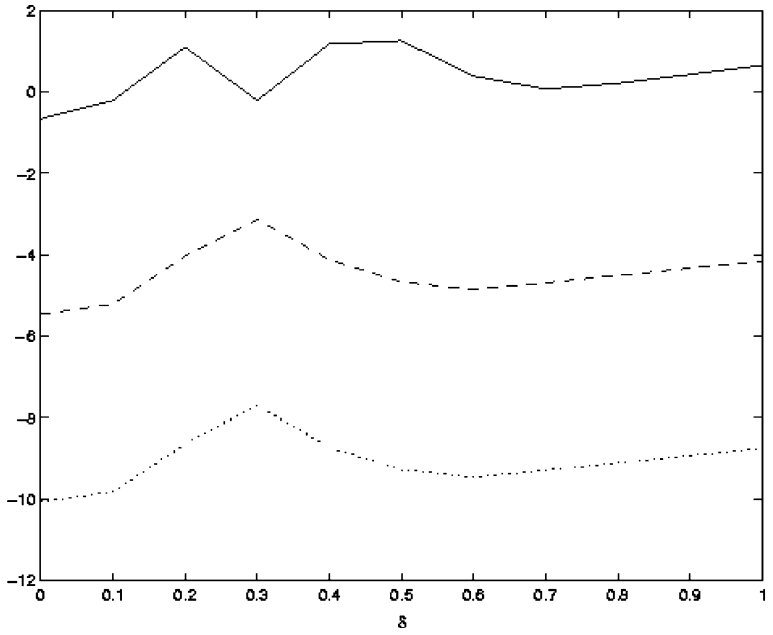

Fig. 4. $Re = 10$, $t = 1$. The logarithm of the maximal error $\log e^{\varepsilon}$ for $\varepsilon = .1$ (solid line), $\varepsilon = .01$ (dashed line), $\varepsilon = .001$ (dotted line) as a function of δ.

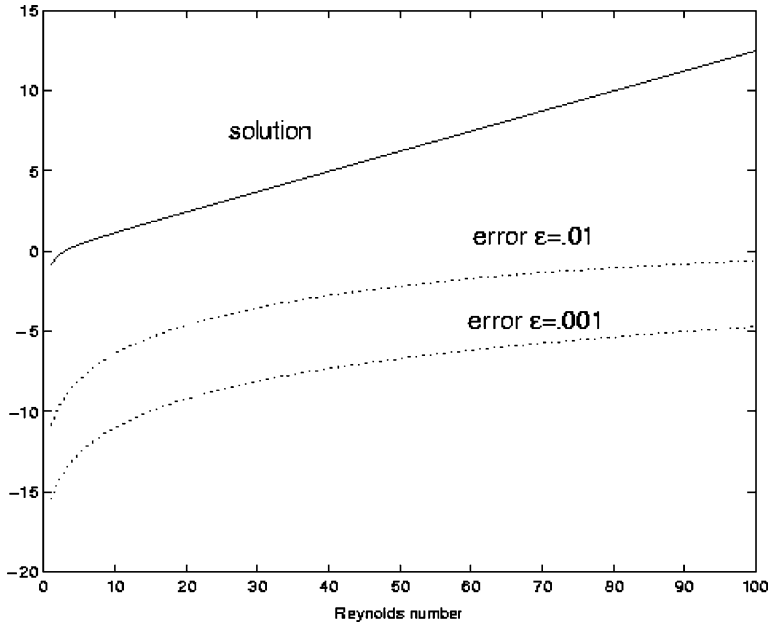

Fig. 5. $t = 1$. Log-scale. The effective coefficient a (solid line), $m = (1,1)/\sqrt{2}$ and the relative error r^{ε} (dotted lines) as a function of Re.

5. Conclusions

The behavior of modulational perturbations (eddy viscosity) of cellular flows was studied numerically for $Re \in [1, 100]$, $\varepsilon = .1, .01, .001$. The effective equations for modulational perturbations predict accurately the solution when the ratio between scales ε is sufficiently small or the Reynolds number Re is not large. More specifically, a priori error estimates from [9] guarantee that the error is expected to be small for our numerical experiments if $\varepsilon Re \leqslant C$, where $C \ll 1$, numerically we observe that the effective equations give an accurate approximation for the behavior of modulational perturbations for the choice of parameters: $\varepsilon Re \leqslant .1$. The designed numerical upscaling algorithm successfully addresses a general issue in time-dependent upscaling: accumulation of error due to time-stepping. This upscaling method can be applied to more general highly oscillatory underlying flows. Its spectral numerical implementation, presented here, can be easily extended to any periodic flow, that satisfies the two dimensional analog of the Beltrami property (2), however this is still very restrictive for applications (see e.g. a review [8] and references therein). The implementation of this method for more physically realistic flows remains to be done.

Acknowledgements

We are grateful to H.-M. Zhou for reading a draft of this paper and making remarks about it. We would also like to thank anonymous referees for their valuable comments.

References

[1] V.I. Arnold, B.A. Khesin, Topological Methods in Hydrodynamics, Applied Mathematical Sciences, 125, Springer, New York, 1998.
[2] A. Bensoussan, J.L. Lions, G.C. Papanicolaou, Asymptotic Analysis for Periodic Structures, North-Holland, Amsterdam, 1978.
[3] B. Dubrulle, U. Frisch, Eddy viscosity of parity-invariant flows, Phys. Rev. A 43 (1991) 5355–5364.
[4] A. Fannjiang, T. Komorowski, Diffusive and nondiffusive limits of transport in nonmixing flows, SIAM J. Appl. Math. 62 (3) (2002) 909–923.
[5] A. Fannjiang, G. Papanicolaou, Convection enhanced diffusion for periodic flows, SIAM J. Appl. Math. 54 (2) (1994) 333–408.
[6] U. Frisch, Z.S. She, P.L. Sulem, Large-scale flow driven by the anisotropic kinetic alpha effect, Physica D 28 (1987) 382–392.
[7] A.M. Matache, I. Babuška, C. Schwab, Generalized p-FEM in homogenization, Numer. Math. 86 (2) (2000) 319–375.
[8] A.J. Majda, P.R. Kramer, Simplified models for turbulent diffusion: theory, numerical modeling, and physical phenomena, Phys. Rep. 314 (4–5) (1999) 237–574.
[9] A. Novikov, Modulational stability of cellular flows, Nonlinearity 16 (2003) 1607–1639.
[10] A. Novikov, G. Papanicolaou, Eddy viscosity of cellular flows, J. Fluid Mech. 446 (2001) 173–198.
[11] A. Novikov, Eddy viscosity of cellular flows, Ph.D. Thesis, Stanford, 1999.
[12] G.I. Sivashinsky, A.L. Frenkel, On negative eddy viscosity under conditions of isotropy, Phys. Fluids A 4 (1992) 1608–1610.
[13] G.I. Sivashinsky, V. Yakhot, Negative viscosity effect in large-scale flows, Phys. Fluids 28 (1985) 1040–1042.
[14] A. Wirth, S. Gama, U. Frisch, Eddy viscosity of three-dimensional flow, J. Fluid Mech. 288 (1995) 249–264.
[15] X.H. Wu, Y. Efendiev, T.Y. Hou, Analysis of upscaling absolute permeability, Discrete Contin. Dyn. Syst. Ser. B 2 (2) (2002) 185–204.